Available online at www.sciencedirect.com

ScienceDirect

JOURNAL OF ORTHOPAEDIC TRANSLATION

ORIGINAL ARTICLE

Restoration of osteochondral defects by implanting bilayered poly(lactide-*co*-glycolide) porous scaffolds in rabbit joints for 12 and 24 weeks

Pingguo Duan [a,☆], Zhen Pan [b,☆], Lu Cao [c], Jingming Gao [b], Haoqun Yao [a], Xiangnan Liu [b], Runsheng Guo [a], Xiangyu Liang [b], Jian Dong [c,**], Jiandong Ding [b,*]

[a] Department of Orthopaedic Surgery, The First Affiliated Hospital of Nanchang University, Nanchang 330006, China
[b] State Key Laboratory of Molecular Engineering of Polymers, Department of Macromolecular Science, Fudan University, Shanghai 200438, China
[c] Department of Orthopaedic Surgery, Zhongshan Hospital, State Key Laboratory of Molecular Engineering of Polymers, Fudan University, Shanghai 200032, China

Abstract *Background:* With the ageing of the population and the increase of sports injuries, the number of joint injuries has increased greatly. Tissue engineering or tissue regeneration is an important method to repair articular cartilage defects. While it has recently been paid much attention to use bilayered porous scaffolds to repair both cartilage and subchondral bone, it is interesting to examine to what extent a bilayer scaffold composed of the same kind of the biodegradable polymer poly(lactide-*co*-glycolide) (PLGA) can restore an osteochondral defect. Herein, we fabricated bilayered PLGA scaffolds and used a rabbit model to examine the efficacy of implanting the porous scaffolds with or without bone marrow mesenchymal stem cells (BMSCs). The present manuscript reports the regenerative potential up to 24 weeks. *Methods:* The osteochondral defect, 4 mm in diameter and 5 mm in depth, was created in the medial condyle of each knee in 23 rabbits. The bilayered PLGA scaffolds with a pore size of 100 —200 μm in the chondral layer and a pore size of 300—450 μm in the osseous layer, seeded with or without BMSCs in the chondral layer, were then transplanted into the osteochondral defect

* Corresponding author. State Key Laboratory of Molecular Engineering of Polymers, Department of Macromolecular Science, Fudan University, No. 2005 Songhu Road, Shanghai 200438, China.
** Corresponding author. Department of Orthopaedic Surgery, Zhongshan Hospital, State Key Laboratory of Molecular Engineering of Polymers, Fudan University, No. 180 Fenglin Road, Shanghai 200032, China.
E-mail addresses: dong.jian@zs-hospital.sh.cn (J. Dong), jdding1@fudan.edu.cn (J. Ding).
☆ These authors contributed equally to this work.

of each knee. The osteochondral defect created in the same manner was untreated to act as the control. At 12 and 24 weeks postoperatively, condyles were harvested and analyzed using histology, immunohistochemistry, real-time polymerase chain reaction, and biomechanical testing to evaluate the efficacy of osteochondral repair.

Results: No joint erosion, inflammation, swelling, or deformity was observed, and all animals maintained a full range of motion. Compared with the untreated blank group, the groups implanting the bilayered scaffolds with or without cells exhibited much better resurfacing, similar to the surrounding normal tissue. The histological scores of neotissues repaired by the scaffold with cells were closer to that of normal tissue. Although the biomechanical properties of neotissues were not as good as the normal tissue, no significant difference was found between the gene levels of neotissues repaired by the scaffold with or without cells and that of the normal tissue. The repair of the osteochondral defect tends to be stable 12 weeks after implantation.

Conclusions: Our bilayered PLGA porous scaffold supports long-term osteochondral repair via *in vivo* tissue engineering or regeneration, and its effect can be further facilitated under the scaffold seeded with allogenic BMSCs.

The translational potential of this article: The bilayered PLGA porous scaffold can facilitate the repair of osteochondral defects and has potential for application in osteochondral tissue engineering.

Introduction

Lacking of blood supply and innervation, articular cartilage has a very limited capacity for self-healing once damaged [1,2]. To treat the cartilage defects, early clinical intervention includes bone marrow stimulation techniques, cartilage plug transplant, and expanded autologous chondrocyte or mesenchymal stem cell implantation [2—4]. Given the limitations of current surgical approaches to treat articular cartilage lesions, tissue engineering has been pursued extensively in recent decades and exhibited promising applications in clinical treatment [5—8]. Synthetic implants can be fabricated using biodegradable and biocompatible materials and formed into porous scaffolds. A variety of scaffolding materials, seeded with or without cells, have been engineered to repair the cartilage defect in animal models [9—11].

Articular cartilage has different biochemical and biomechanical properties compared with the subchondral bone, so layered porous scaffolds have been designed to better provide the different environments for the chondrocytes and osteoblasts [12—14]. So far, most of the layered scaffolds have been made of two or more different biomaterials. The layered scaffold fabricated with only one raw biomaterial is relatively less reported, and the corresponding investigation of such a simple scaffold system has its own right. Poly(lactide-*co*-glycolide) (PLGA) is a very useful biodegradable polymer owing to its tunable biodegradation rate, very good mechanical and processing properties, and so on [15—17]. PLGA was previously used to fabricate the integrated bilayered scaffolds by adjusting the different pore sizes or different porosities in the chondral and osseous layers. The results found that bilayered PLGA scaffolds with different pore sizes or porosities, seeded with or without bone marrow mesenchymal stem cells (BMSCs), promoted the simultaneous regeneration of articular cartilage and subchondral bone in different degrees in rabbits [18,19].

The pore size and porosity of a scaffold play vital roles in osteochondral tissue engineering. Scaffolds with a pore size of 100—200 μm in the chondral layer and a pore size of 300—450 μm in the osseous layer displayed the best effect on repairing the osteochondral defect [20]. It might be the compatible mechanical property of the type of a bilayered scaffold that led to its good restoration efficacy. The mechanical property of the scaffold is one of the vital issues when promoting bone and cartilage tissue regeneration [21]. The modulus of scaffolds should match the biomechanics of repaired tissues, which is especially important for stratified tissues connecting together. Cartilage is a highly hydrated composite with relatively low compressive stiffness, whose instantaneous compressive Young's modulus is 1.36—39.2 MPa [22]. The subchondral bone and the cancellous bone have the compressive modulus in the range of 1.4—9800 MPa [22—24]. Although the bilayered PLGA scaffold was confirmed to partially repair the osteochondral defect at 12 weeks after implantation [20,24], the repairing effect and the biomechanical property of the neotissue in a longer time remained an open question.

The aim of the present study is to fabricate the integrated bilayered PLGA scaffolds with appropriate porosities of the two layers (pore size of 100—200 μm in the chondral layer and pore size of 300—450 μm in the osseous layer) and then to observe the long-term repairing effect by implanting the bilayered scaffolds seeded with or without BMSCs in rabbits (Figure 1), including estimation of the biomechanical properties of the neotissues.
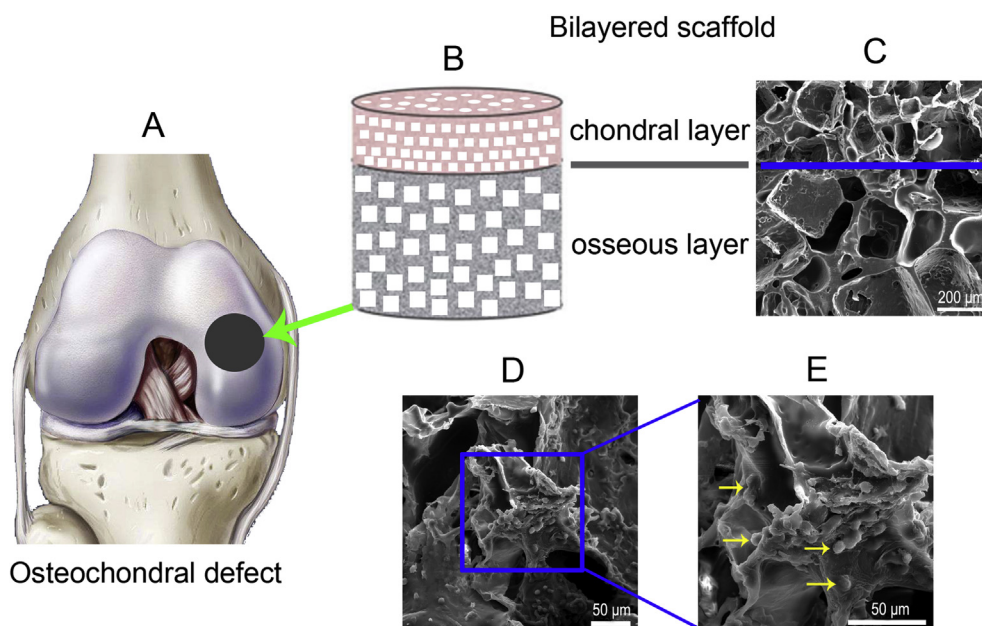
Figure 1 (A) Schematic of the osteochondral defect of the medial condyle in the knee joint, as indicated by the black circle. (B) Diagram of a bilayered PLGA scaffold. (C) Pore structure of the bilayered PLGA scaffold observed via SEM. The blue line indicates the boundary of the two layers. (D) An SEM image of BMSCs on the internal surfaces of the chondral layer of the porous scaffold after being cultured for one week. (E) Magnification of the rectangle of (D). The yellow arrows indicate cells adhered to the pore wall of the scaffold. BMSCs = bone marrow mesenchymal stem cells; PLGA = poly(lactide-*co*-glycolide); SEM = scanning electron microscopy.

Materials and methods

Ethics statement

We carried out all animal experiments under anaesthesia with ketamine hydrochloride. We have made efforts to minimize suffering, following the Guide for the Care and Use of Laboratory Animals of the National Institutes of Health. The protocol of animal experiments has been approved by the Ethics Committee of Animal Experiments at Nanchang University.

Preparation of integrated bilayered PLGA scaffolds

The raw copolymer of PLGA was PLGA85/15, with a molar ratio of lactide/glycolide (LA/GA) of 85/15. It was a product of Purac Co. (Netherlands) with an inherent viscosity of 2.36 dl/g. A room-temperature compression molding/particulate leaching method developed by Ding et al [17,25,26] was used to fabricate PLGA porous scaffolds, in which dichloromethane was used as the solvent to dissolve PLGA and sodium chloride (NaCl) particulates with size ranges of 100−200 μm and 300−450 μm were used as a porogen.

In brief, we mixed the PLGA solution and porogen and then pressed the mixture into a predesigned mold. After keeping the pressure for a while, we released the mold and obtained a cylindrical prescaffold. We then glued two prescaffolds (shaped mixtures of PLGA with porogens of different pore sizes) with dichloromethane. After trimming the glued prescaffold, we put it into water to dissolve the water-soluble porogen, until no Cl$^-$ could be detected significantly in the medium. Eventually, integrated bilayered PLGA scaffolds were obtained after porogen leaching and drying.

BMSC culture

We obtained BMSCs from New Zealand white rabbits. Briefly, according to the previous protocol [27], 5 mL of a blood sample was harvested from bone marrows of rabbits with 1 mL of heparin (1000 units/1 mL) through penetration of the posterior surface of the cortex of the iliac crest using an 18-gauge needle. The blood sample was centrifuged for 5 min, and the resultant supernatant was discarded. The isolated cell pellets were resuspended in 5 mL of Dulbecco's modified Eagle's medium with low glucose (Gibco, Massachusetts, USA), containing 10% deactivated foetal bovine serum (Gibco, Australia) and 1% antibiotics (penicillin and streptomycin).

We seeded the cells in T-25 flasks (Corning, New York, USA), which were kept in an incubator (37 °C and 5% CO_2). The culture medium was changed every 3 days. After the proliferated cells got 80% confluence, we detached cells by treatment with 0.25% trypsin and ethylenediaminetetra-acetic acid (Sigma, Missouri, USA). The detached cells were subcultured at a ratio of 1:3. BMSCs of passage 3 were used in the following experiments.

BMSC seeding

Before cell and animal experiments, PLGA porous scaffolds were sterilized with ethylene oxide. We put the sterilized scaffolds in 24-well culture plates (Corning).

To improve cell seeding efficiency, we first had cells incubated in Dulbecco's modified Eagle's medium with low glucose overnight. Then, we used a 1-cc syringe to evenly seed a cell suspension (24 mL) into the chondral layer of the bilayered scaffold. The loaded cells were allowed to adhere to the scaffold during the first 2 h of culture before the addition of 1 mL fresh complete medium. The cell culture medium was then changed every 3 days.

For *in vitro* experiments, cell-seeded scaffolds (5×10^5 cells per scaffold) were cultured in fresh complete medium. For *in vivo* experiments, cell-seeded scaffolds (1×10^6 cells per scaffold) were cultured in the same medium under standard conditions for 7 days, before implantation.

Morphology observations

The pore morphology in the porous scaffold and cells on the pore walls were observed via scanning electron microscopy (SEM). After 7 days of culture, the cell-seeded scaffolds were analyzed under SEM (TS5136MM; TESCAN, Brno, Czech) and fluorescence microscopy (Olympus BX51, Tokyo, Japan). Before observations, we fixed the cells in the scaffolds in 2.5% glutaraldehyde at 4 °C for 24 h. Thereafter, the samples were sequentially dehydrated, critical point—dried, and sputter-coated with gold. The pretreated samples were then observed by SEM.

Live/dead cell staining

To determine cell viability within the scaffold, the cell-seeded scaffolds (5×10^5 cells per scaffold) were stained using the Live/Dead Cell Staining Kit (BioVision, California, USA) 7 days after being cultured, according to the manufacturer's instructions. Briefly, the cell-seeded scaffolds were incubated with 500 μL of the Live/Dead reagent for 15 min in an incubator (37 °C and 5% CO_2) and then viewed by fluorescence microscopy.

Surgical implantation

In this study, 23 skeletally mature rabbits were sacrificed. Each rabbit was 5—6 months old and weighed 2.9—3.5 kg. We used a surgical drill bit to generate osteochondral defects centred on the medial femoral condyles. Each defect was 4 mm in diameter and 5 mm in depth. We then press-fitted the PLGA scaffolds into the osteochondral defects randomly. Some of the scaffolds were seeded with BMSCs in the chondral layer ($n = 17$).

The bilayered PLGA scaffolds with or without cells were pre-set up as one implanted pair. Rabbit knee joints were assigned randomly to the implants of two pairs in 23 rabbits (12 weeks and 24 weeks, $n = 6$ for each scaffold group; 24 weeks, $n = 5$ biomechanical testing for each scaffold group). Besides, the untreated lateral condyle was used as a normal group; and some medial condyle defects in the same knee joints remained blank, which served as a blank control group (12 knees, $n = 6$).

In the forthcoming days after operation, we still fed rabbits with tap water and food ad libitum. The animals were allowed to move freely in cages. We injected gentamycin (4 mg/kg) intramuscularly for 3 days after surgical implantation, which is critically important for avoiding infection.

Tissue retrieval and histological analysis

At 12 and 24 weeks postoperatively, we injected ketamine hydrochloride to sacrifice rabbits and took samples from the repaired or originally defected site. Each sample was photographed and harvested. For 24-week samples, five of them were used for biomechanical tests. We then divided the remaining samples into two halves: one half was for subsequent real-time polymerase chain reaction (PCR) and thus quickly frozen in liquid nitrogen; the other half was for histological observations and immunohistochemical assessment, and thus experienced paraffin sectioning. The sections were stained with haematoxylin and eosin, toluidine blue, or safranin O/fast green for histological observations. The quality of the repaired tissue was evaluated by two blinded independent individuals in the light of histological grading scale described by Wakitani et al. [28].

As the immunohistochemical assessment is concerned, the paraffin sections were first deparaffinized and rehydrated and then were blocked with 10% goat serum at 25 °C for 20 min. The blocked sections were incubated with 10 μg/mL anti—collagen type I or anti—collagen type II mouse monoclonal antibody (EMD Millipore, Massachusetts, USA) at 4 °C overnight. We used phosphate buffer saline solution to wash samples. The washed sections were incubated with biotinylated goat anti—mouse secondary antibody (DAKO, California, USA) at 37 °C for 20 min. We eventually visualized immunoreactivity after treating the sections in 3,3′-diaminobenzidine tetrahydrochloride solution (0.5 mg/mL); The 3,3′-diaminobenzidine tetrahydrochloride was dissolved in Tris-HCl buffer (pH 7.6), with 0.01% H_2O_2 added.

Real-time PCR

PCR was used to semiquantify the gene expression of some target proteins. We first homogenized samples using a tissue tearor. TRIzol reagent (Invitrogen, California, USA) was used to isolate total RNA. Then, a reverse transcription system (TaKaRa, Japan) was used to reverse transcribe cDNA.

PCR was performed using Brilliant SYBR Green QPCR master mix (TaKaRa, Japan) in an ABI 9700 real-time PCR system (LabX, Midland, Canada) under the conditions of 15 s at 95 °C and 1 min at 60 °C. Forty cycles of the fluorescence intensity were recorded. This study examined the genes of collagen I and collagen II. The expression level of glyceraldehyde 3-phosphate dehydrogenase was used to normalize that of each target gene. Each group was replicated at least three times.

Biomechanical testing

The neotissues of 4-mm diameter and 5-mm height were taken from the osteochondral defect using the surgical drill bit and then harvested. The compressive moduli of the neotissues were characterized by measurement of stress—strain curves at room temperature, similar to our previous work [24,29]. The samples were tested on a SANS CMT4104 (Shenzhen, China) testing machine. The

neotissues were compressed at a speed of 6.0 mm/min. The normal tissues were harvested and tested as a positive control.

Statistical analysis

All data are expressed as mean $\pm$ standard deviation. The histological grading and so on were analyzed using Student's t tests (for each two of the groups). The significant level was set as $p < 0.05$.

Results

Characterization of as-prepared bilayered scaffolds

The integrated bilayered PLGA scaffolds, which were 4 mm in diameter and 5 mm in height (chondral layer, 1 mm and osseous layer, 4 mm), were fabricated successfully. The cylinder scaffolds consisted of two layers with different pore sizes (100—200 μm in the chondral layer and 300—450 μm in the osseous layer) as assessed by SEM (Figure 1). The porosities of both layers were approximately 85% in both layers, as determined by the content of porogen used for fabrication of the porous scaffolds [30].

Observation of seeded BMSCs on the scaffold *in vitro*

BMSCs were uniformly distributed on the scaffold pore wall with deposition of extracellular matrix, as observed via SEM (Figure 1D and E). The survival of the BMSCs within the scaffolds over a 7-day period was assessed using the Live/Dead assay with a fluorescence microscope. Most of the adhered BMSCs were viable, and only a few dead cells were observed, as indicated in Figure 2.

Here, we would like to mention that fewer cells were seeded for *in vitro* experiments than for *in vivo*. That is the usual way in the corresponding studies. In vitro, one seeds relatively fewer cells to enable observations of cells on the scaffold wall via SEM and fluorescence microscopy. *In vivo*, one usually seeds more BMSCs to enhance cell gathering and differentiating into chondrocytes.

Global observation

None of the rabbits could not tolerate the operations in our study. The animals were found to be ambulatory immediately after recovery from anaesthesia. According to our global view, no significant inflammation was observed in the synovial membrane or other joint tissues in and around the knee joint.

In the blank control group, the obvious vacancy defect could still be seen in the centre of the condyle 24 weeks after operations ($n = 6$), indicating poor self-repair ability for a defect over critical size, as reported in previous studies [31,32]. The defects with implanted scaffolds were covered with an irregular tissue at 12 weeks. At 24 weeks, the medial condyles were repaired by the bilayered PLGA scaffolds with or without cells. The neotissues in the cell-seeded bilayered scaffolds exhibited better resurfacing than those in the scaffolds without cells 24 weeks after implantation (Figure 3).

Histological examination

In the light of histological grading scores, as described by Wakitani et al. [28], a lower score reflects a better repair. At 12 and 24 weeks after implantation, the scores of tissues repaired by scaffolds with cells were lower than those of tissues repaired merely by scaffolds, and the scores of tissues repaired by scaffolds with or without cells were lower than those of tissues in the blank group ($p < 0.05$) (Figure 4). Although the scores of tissues repaired by scaffolds with cells were higher than the score of the normal tissue, the difference was not distinct ($p > 0.05$). The difference between the 12-week scores and 24-week scores was also insignificant, suggesting that the repair of the osteochondral defect tends to be stable 12 weeks after implantation.

The histological images of repaired tissues 12 weeks and 24 weeks after implantation are shown in Figure 5 for groups of porous PLGA scaffolds preloaded with or without BMSCs. In the blank control group, the defects could not be self-repaired as our previous studies [20,24], so the data of histological staining are not shown. At 12 weeks after implantation, most sections showed that the scaffold
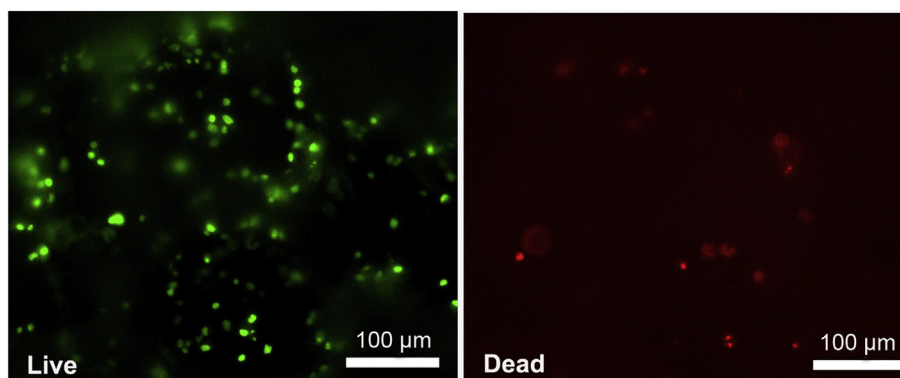

Figure 2 Fluorescence micrographs of BMSCs on the chondral layer of porous scaffolds after 7 days of culture in the basal medium. Using the Live/Dead assay kit, it was found that the majority of the adhered BMSCs were viable, as indicated by green fluorescence, with only a few dead cells as indicated by red fluorescence. BMSCs = bone marrow mesenchymal stem cells.
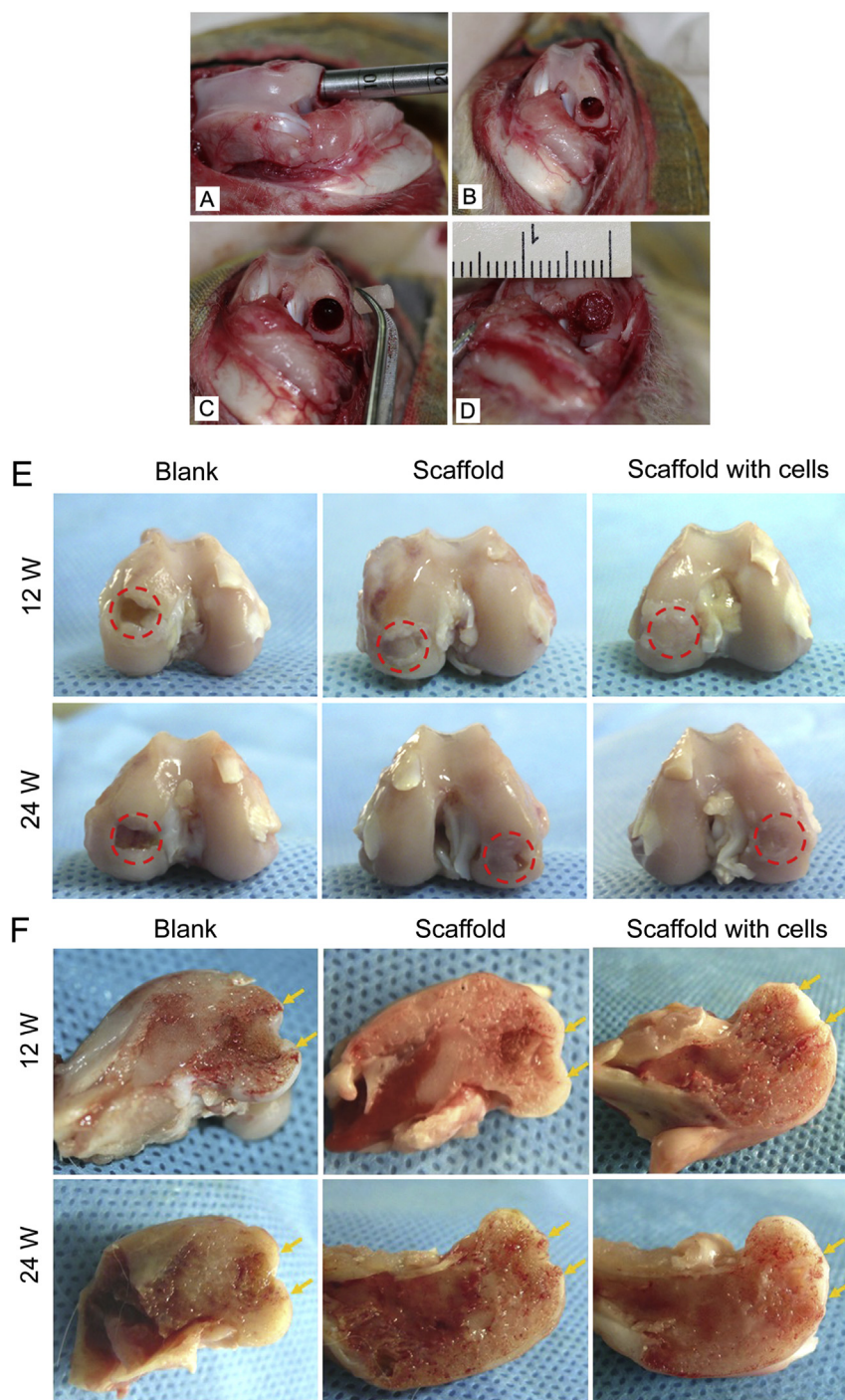
Figure 3 (A–D) Photographs of osteochondral defects created in rabbit knee joints. (A) A defect was created in the medial femoral condyle by applying a surgical drill bit; (B) the defect was 4 mm in diameter and 5 mm in thickness in the medial condyles of the knee joint; (C and D) the medial condyle defect was implanted with the bilayered PLGA scaffold seeded with BMSCs. (E) The global and cross-sectional views of reparative tissues 12 weeks after implantation. (F) The global and cross-sectional views of reparative tissues 24 weeks after implantation. The red circles in (E) indicate the original defect region. The yellow arrows in (F) indicate the interfaces between the neotissues and native osteochondral tissues. At 12 weeks, the defects in the medial condyles were repaired with a bilayered PLGA scaffold with or without cells. The defects were covered with an irregular tissue. The obvious vacancy defect could be seen in the blank control group at 12 and 24 weeks after operations. At 24 weeks, the neotissue in the condyle-implanted cell-seeded scaffold exhibited better resurfacing than that in the condyle-implanted scaffold, as indicated by the red dotted rings in the defect sites.
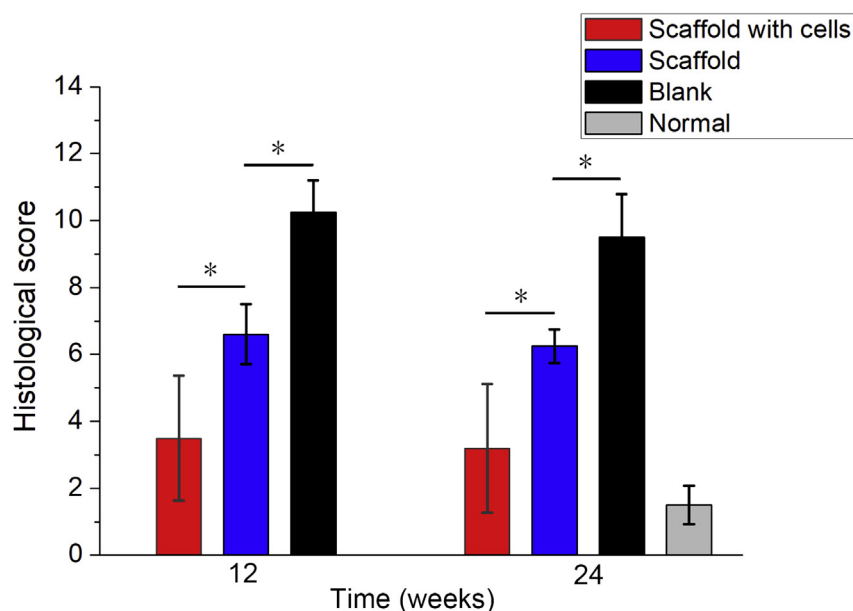
Figure 4   Histological scores for reparative tissues. The histogram shows that the scores of tissues repaired by scaffolds with or without cells were lower than those of tissues in the blank group, and the scores of tissues repaired by scaffolds with cells were both lower than those of tissues repaired by scaffolds at 12 weeks and 24 weeks after implantation ("*": $p < 0.05$). And the scores of tissues repaired by scaffolds with or without cells were higher than the score of the normal tissue. The difference between the group of scaffold with cells and the normal tissue was not significant ($p > 0.05$). The scores between 12 and 24 weeks for each group did not exhibit a significant difference ($p > 0.05$).

materials degraded in different degrees, and the neotissues were well integrated with the surrounding osteochondral tissues. At 24 weeks, for bilayered scaffolds with cells, reparative tissues had a higher percentage of hyaline cartilage and better bone regeneration compared with bilayered scaffolds without cells from haematoxylin and eosin, toluidine blue, and safranin O/fast green staining, in which there was a visible tidemark between cartilage layer and subchondral bone layer (Figure 5).

Some typical immunohistochemical images are shown in Figure 6. The chondral region exhibited stronger expression of collagen type II, and the subchondral region was rich in collagen type I. From histological staining, it was found that the formed cartilage layer was thicker than the native cartilage at 12 weeks. The thickness of cartilage was about 1.5 mm in the group of scaffold with cells and 1.0 mm in the scaffold group. The thickness of cartilage was almost or less than 0.5 mm at 24 weeks, while the thickness of the normal cartilage was almost 0.3—0.5 mm. After 24 weeks, although the neotissues regenerated by bilayered scaffolds with cells were better than those repaired by bilayered scaffolds without cells, the thickness of the chondral region was declined and closer to that of the native cartilage (Figures 5 and 6).

Analysis of gene expression

We further used real-time PCR to semiquantify the pertinent gene expression of the neotissues repaired by the scaffold with or without cells at 12 and 24 weeks after implantation (Figure 7). After 24 weeks, the relative level of collagen type I in the scaffold group was higher than that

in other groups, leading to a larger variation of the measured value, and the relative level of collagen type II in the group of scaffold with cells was higher than that in other groups, close to that of the normal group.

Biomechanical test

The mean Young's moduli of the repaired tissues in scaffolds with or without cells treated were 91.2 MPa for the scaffold with cells and 28.9 MPa for the scaffold ($n = 5$). The stiffness was less than that of normal cartilage (mean Young's modulus, 176.9 MPa). There was a significant difference between repaired tissues of the group of scaffold and the group of scaffold with cells ($p < 0.05$).

From the compression test, the Young's moduli of repaired tissues from the group of scaffold with cells was about half of that of normal cartilage at 24 weeks postoperatively (Figure 8). Although after 24-week implantation, the stiffness of neotissues did not fully meet the physiological property of the normal articular cartilage, yet the biomechanical tests outputted the same order of magnitude as that of normal osteochondral tissue.

Discussion

With the development of biomaterials and tissue engineering, the regenerative research of osteochondral defects has been paid much attention. In recent years, osteochondral tissue engineering or tissue induction with porous scaffolds has been tried to repair cartilage injury, and stratified scaffolds have been used to mimic cartilage and subchondral bone layers [15,32,33]. Most of the
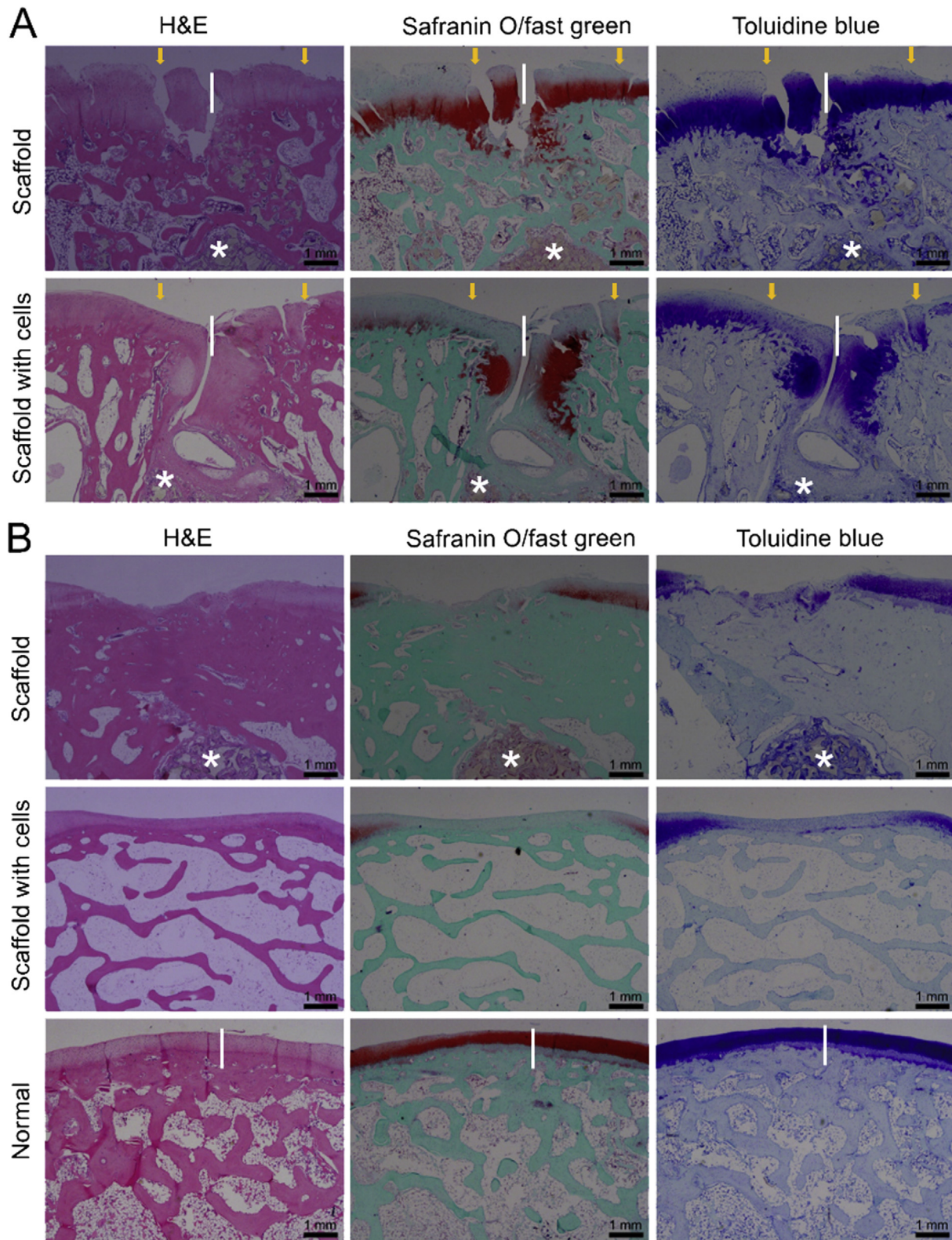
Figure 5 (A) The histological images of repaired tissues 12 weeks after implantation; (B) the histological images of repaired tissues 24 weeks after implantation (H&E, safranin O/fast green, and toluidine blue staining). The length of the white vertical line is 1 mm, which is used to measure the thickness of the cartilage. The white asterisks indicate the remnant scaffold materials. H&E = haematoxylin and eosin.
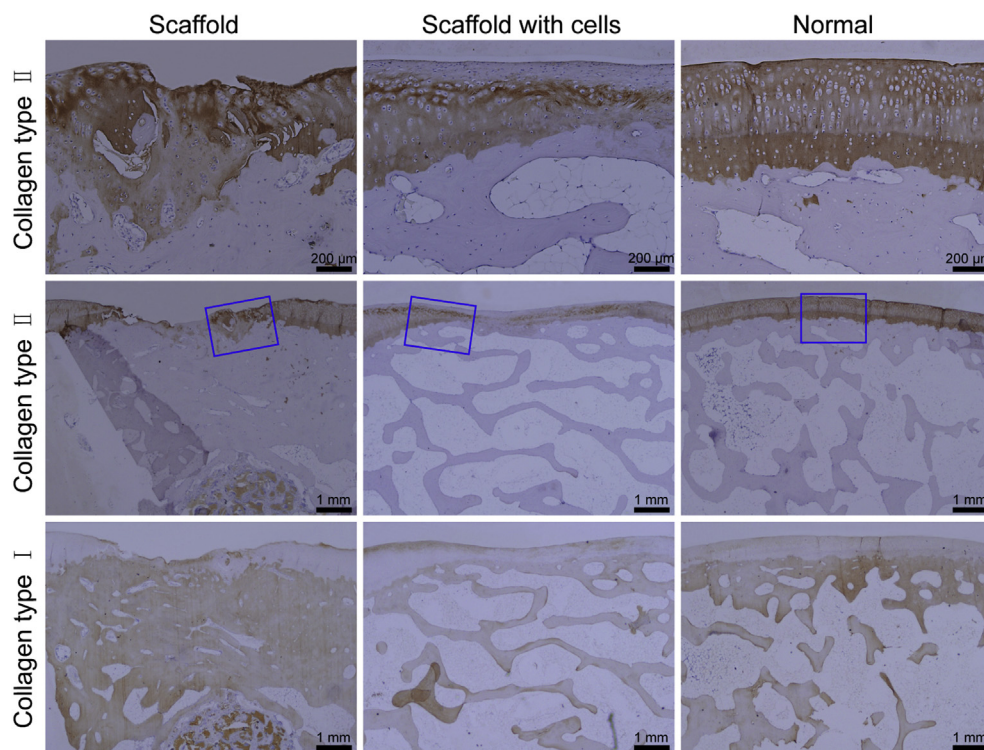
Figure 6 Immunohistochemical images of tissues 24 weeks after implantation. For collagen type II, the expression in the chondral region of tissues repaired and of the normal tissue was positive. The images in the first row come from magnification of the blue rectangles in groups of scaffold, scaffold with cells, and normal, respectively. For collagen type I, the expression in the subchondral region of tissues repaired and of the normal tissue was positive.

stratified scaffolds were fabricated by composite bio-materials for repair of the osteochondral defect [7,21]. Although certainly an incorporation of natural extracellular matrix (ECM) into biomaterial scaffolds can promote repair of cartilage and soft tissues [34—37], we used, in this study, merely synthetic PLGA to fabricate the integrated bilay-ered scaffold, which was made of the same raw material yet had different pore sizes between the chondral layer and subchondral layer to mimic the different mechanical properties of cartilage and subchondral bone. From the results of this study, PLGA bilayered scaffolds seeded with BMSCs in the chondral layer supported the simultaneous regeneration of cartilage and subchondral bone in rabbits. The osteochondral defects were resurfaced from the macroscopic view of the femoral condyle at 12 and 24 weeks after implantation.

We have fabricated a series of PLGA bilayered scaffolds with different pore sizes and porosities between the two layers [15,20,24]. These types of scaffolds seeded with allogenic BMSCs in the chondral layer repaired the osteo-chondral defects of rabbits to different extents, exhibiting effects of pore sizes and porosities on the restoration of the osteochondral defect. In the present study, we fabricated bilayered PLGA scaffolds that had a pore size of 100—200 μm in the chondral layer, pore size of 300—450 μm in the osseous layer, and 85% porosity in both layers. The scaffolds were seeded with allogenic BMSCs in the chondral layer to repair the osteochondral defect in rabbits. SEM observations showed that BMSCs spread well on the scaffold pore walls. Using the Live/Dead assay, it was found that the

majority of the adhered BMSCs were viable in the scaffold. We confirmed that the PLGA scaffold had good biocom-patibility and facilitated the chondrogenesis of BMSCs [29,38].

The *in vivo* repair of osteochondral defects by scaffolds with BMSCs was better than that by scaffolds without BMSCs, in accordance with the previous studies [20,24]. Furthermore, by tracking implanted BMSCs in our previous study, it had been proved that BMSCs could survive at least 6 weeks *in vivo* [20]. These findings suggested that allogenic BMSCs promote remarkably the regeneration of cartilage, while simply implanting an appropriate porous scaffold had much better efficacy than the untreated group. Although the osseous layer of the scaffold was not seeded with BMSCs, the formation of trabecular bone was found under the subchondral region, which might arise from endogenous cell homing or internal environment.

From the results of histology, the blank control group showed very limited osteochondral regeneration. The bilayered scaffold facilitated the regeneration of cartilage and bone. The repairing effect of the bilayered scaffold with or without cells tended to be stable after 12 weeks of implantation (Figures 4 and 5). The neotissues integrated well with the surrounding tissues, and a visible tidemark could be found between the cartilage layer and sub-chondral bone layer (Figure 6).

We also observed that the hyaline-like cartilage in the defects was less than the normal cartilage, and the height of the newly formed cartilage layer was more than the native cartilage at 12 weeks, nearly flat with the normal at
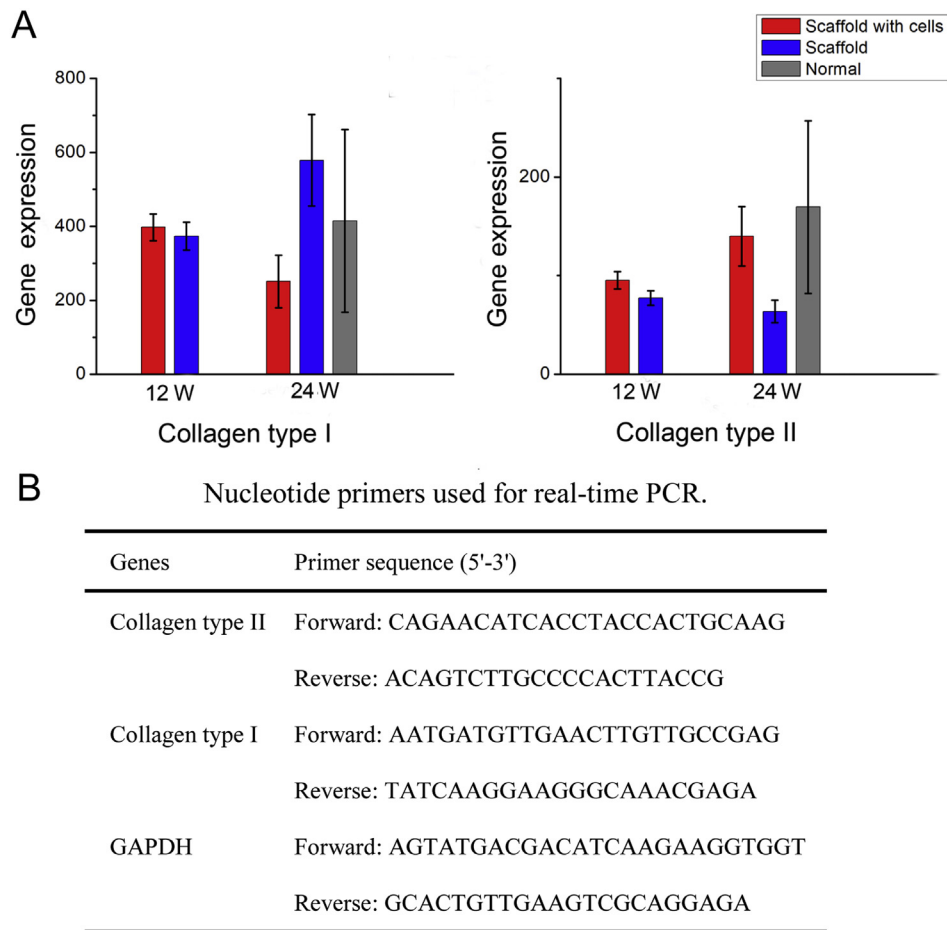
Figure 7 (A) The relative levels of collagen type II and type I were assessed with real-time PCR in each group. For collagen type I, the relative level in the scaffold group at 24 weeks after implantation was higher than that in other groups. For collagen type II, the relative level in the scaffold with cells group at 24 weeks after implantation was higher than that in other groups, close to that of the normal group. GAPDH expression was used for normalization. All values are expressed as mean $\pm$ SD. (B) Nucleotide primers used for real-time PCR. GAPDH = glyceraldehyde 3-phosphate dehydrogenase; PCR = polymerase chain reaction; SD = standard deviation.
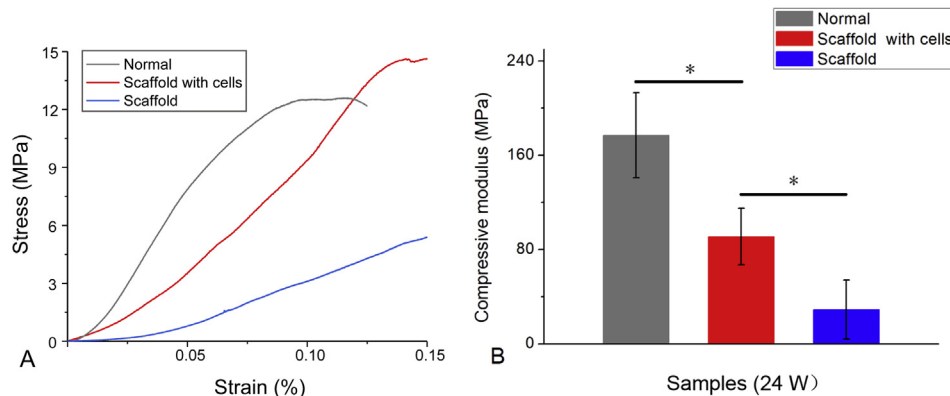

Figure 8 (A) Typical stress—strain curve of repaired tissues and normal osteochondral tissues. (B) The compressive moduli in the groups of scaffolds with and without cells and normal osteochondral tissues. $n = 5$; "*": $p < 0.05$.

24 weeks. One of the reasons may be the partial in-compatibility so that the formation of neotissues did not

well match the degradation of PLGA scaffolds. According to the histological sections, the remnant of the PLGA scaffold

was found in the subchondral region at 12 weeks after implantation, but was sparse in some samples at 24 weeks. The degradation rate of the biomaterial can influence the adhesion and differentiation of mesenchymal stem cells [39] and then compromise the tissue repair. Another vital reason might be partial biomechanical discordance of neotissues in the defects and the implanted bilayered scaffolds.

PLGA bilayered scaffolds seeded with BMSCs could promote the repair of critical-sized osteochondral defects in high load-bearing sites at 6 months or 24 weeks postoperatively. The Young's modulus of neotissue was 91.2 MPa, nearly half of that of the normal cartilage (176.9 MPa). The biomechanical testing showed less satisfactory compressive modulus and stiffness of the regenerated tissues. Besides the quality of the regenerated tissue, another reason may be the improper method of harvesting samples that we used, the surgical drill bit for tissue retrieval, which could destroy the integrity of the neotissue with the strong normal tissue. The compressive modulus and stiffness of the neotissue might be higher if the biomechanical testing was performed on the neotissue *in situ*.

In addition, the maintenance of cartilage homoeostasis is greatly dependent on the interplay between articular cartilage and subchondral bone underneath [40]. Subchondral bone provides a mechanical support for the upper layer cartilage and adapts to respond to the changes in the mechanical environment by modelling and remodelling [41]. While the scaffold led to some articular cartilage repair, implantation of a cell-laden bilayered scaffold was found to further increase cartilage formation in the chondral layer of the scaffold. Despite these improvements, the subchondral bone progressed into the chondral regions of these implants by means of endochondral ossification according to the histological observation at the later stage, which led to thinning of the cartilage tissue [42].

Our results are consistent with the reports of osteochondral repair by bilayered scaffolds and BMSCs [32,38]. Shao et al. evaluated the repair potential in large osteochondral defects with porous polycaprolactone (PCL) for the cartilage and tricalcium phosphate (TCP)-PCL for the bone portion on high load-bearing sites in rabbits. Samples from both the control and experimental groups (PCL/PCL-TCP with BMSCs) had inferior stiffness values to normal unoperated cartilage at 3 months postoperatively ($p < 0.05$), and there was no significant difference between the experimental group and normal unoperated cartilage at 6 months postoperatively [43]. Jiang et al. fabricated a bilayered cylindrical porous plug of PLGA as the chondral phase and PLGA combined with β-TCP as the osseous layer, seeded with chondrocytes, to repair the osteochondral defect in pigs. At 6 months after implantation, the average peak stress was 3.77 MPa for the experimental group and 5.17 MPa for the native cartilage, representing the viscoelastic stiffness of these specimens [44]. Recently, the effect of decellularized cartilage-derived matrix scaffolds and cartilage-derived matrix with calcium phosphate was investigated for the repair of osteochondral defects in horse. Biomechanical testing showed that the repaired tissue was very soft, and the stiffness was significantly less than that of normal adjacent cartilage [45], similar to our results.

The mechanical characteristics of neotissues are difficult to regularize and are influenced by many compound factors, such as test point of the repaired tissue, the models of testing, different animals, and specific conditions of the joint. Anyway, the mechanical quantities of the neotissues were on the same order of magnitude as that of normal articular cartilage in this study.

Conclusions

The bilayered porous scaffolds with different pore sizes in the layers of cartilage and subchondral bone were fabricated using the same raw biodegradable polymer PLGA. The integrated scaffold was confirmed to support the partial regeneration of articular cartilage *in vivo* with 12-week and 24-week observations in a rabbit joint model. The repair efficacy was further improved by the scaffold seeded with allogenic BMSCs in the chondral layer, and the biomechanical tests outputted the same order of magnitude as that of the normal osteochondral tissue. This study illustrates that both 12 weeks and 24 weeks have resulted in partial regeneration of osteochondral defects. Nevertheless, it does not rule out the necessity of even longer *in vivo* observations. The efficacies of 3−5 years are expected in the future.

Conflicts of interest

The authors have no conflicts of interest to disclose in relation to this article.

Acknowledgements

References

[1] Huang BJ, Hu JC, Athanasiou KA. Cell-based tissue engineering strategies used in the clinical repair of articular cartilage. Biomaterials 2016;98:1−22.

[2] Makris EA, Gomoll AH, Malizos KN, Hu JC, Athanasiou KA. Repair and tissue engineering techniques for articular cartilage. Nat Rev Rheumatol 2015;11(1):21−34.

[3] Crist BD, Stoker AM, Pfeiffer FM, Kuroki K, Cook CR, Franklin SP, et al. Optimising femoral-head osteochondral allograft transplantation in a preclinical model. J Orthop Translat 2016;5:48−56.

[4] Li L, Yu F, Zheng L, Wang R, Yan W, Wang Z, et al. Natural hydrogels for cartilage regeneration: modification, preparation and application. J Orthop Translat 2018:1−16. https://doi.org/10.1016/j.jot.2018.09.003.

[5] Lee CH, Cook JL, Mendelson A, Moioli EK, Yao H, Mao JJ. Regeneration of the articular surface of the rabbit synovial joint by cell homing: a proof of concept study. Lancet 2010; 376(9739):440−8.

[6] Fisher MB, Henning EA, Soegaard NB, Dodge GR, Steinberg DR, Mauck RL. Maximizing cartilage formation and integration via a trajectory-based tissue engineering approach. Biomaterials 2014;35(7):2140–8.

[7] Levingstone TJ, Thompson E, Matsiko A, Schepens A, Gleeson JP, O'Brien FJ. Multi-layered collagen-based scaffolds for osteochondral defect repair in rabbits. Acta Biomater 2016;32:149–60.

[8] Zhang YT, Niu J, Wang Z, Liu S, Wu JQ, Yu B. Repair of osteochondral defects in a rabbit model using bilayer poly(lactide-co-glycolide) scaffolds loaded with autologous platelet-rich plasma. Med Sci Mon Int Med J Exp Clin Res 2017; 23:5189–201.

[9] Cao L, Yang F, Liu GW, Yu DG, Li HW, Fan QM, et al. The promotion of cartilage defect repair using adenovirus mediated Sox9 gene transfer of rabbit bone marrow mesenchymal stem cells. Biomaterials 2011;32(16):3910–20.

[10] Dai WD, Kawazoe N, Lin XT, Dong J, Chen GP. The influence of structural design of PLGA/collagen hybrid scaffolds in cartilage tissue engineering. Biomaterials 2010;31(8):2141–52.

[11] Fan HB, Hu YY, Zhang CL, Li XS, Lv R, Qin L, et al. Cartilage regeneration using mesenchymal stem cells and a PLGA-gelatin/chondroitin/hyaluronate hybrid scaffold. Biomaterials 2006;27(26):4573–80.

[12] Zhang SP, Chuah SJ, Lai RC, Hui JHP, Lim SK, Toh WS. MSC exosomes mediate cartilage repair by enhancing proliferation, attenuating apoptosis and modulating immune reactivity. Biomaterials 2018;156:16–27.

[13] Liang XY, Duan PG, Gao JM, Guo RS, Qu ZH, Li XF, et al. Bilayered PLGA/PLGA-HAp composite scaffold for osteochondral tissue engineering and tissue regeneration. ACS Biomater Sci Eng 2018;4(10):3506–21.

[14] Chen GP, Sato T, Tanaka J, Tateishi T. Preparation of a biphasic scaffold for osteochondral tissue engineering. Mater Sci Eng C 2006;26(1):118–23.

[15] Pan Z, Ding JD. Poly(lactide-co-glycolide) porous scaffolds for tissue engineering and regenerative medicine. Interface Focus 2012;2(3):366–77.

[16] Cui SQ, Yu L, Ding JD. Semi-bald micelles and corresponding percolated micelle networks of thermogels. Macromolecules 2018;51(16):6405–20.

[17] Wu LB, Ding JD. In vitro degradation of three-dimensional porous poly(D,L-lactide-co-glycolide) scaffolds for tissue engineering. Biomaterials 2004;25(27):5821–30.

[18] Liang XY, Qi YL, Pan Z, He Y, Liu XN, Cui SQ, et al. Design and preparation of quasi-spherical salt particles as water-soluble porogens to fabricate hydrophobic porous scaffolds for tissue engineering and tissue regeneration. Mater Chem Front 2018;2(8):1539–53.

[19] Dai YK, Shen T, Ma L, Wang DG, Gao CY. Regeneration of osteochondral defects in vivo by a cell-free cylindrical poly(lactide-co-glycolide) scaffold with a radially oriented microstructure. J Tissue Eng Regenerat Med 2018;12(3): e1647–61.

[20] Duan PG, Pan Z, Cao L, He Y, Wang HR, Qu ZH, et al. The effects of pore size in bilayered poly(lactide-co-glycolide) scaffolds on restoring osteochondral defects in rabbits. J Biomed Mater Res A 2014;102(1):180–92.

[21] Yan LP, Silva-Correia J, Oliveira MB, Vilela C, Pereira H, Sousa RA, et al. Bilayered silk/silk-nanoCaP scaffolds for osteochondral tissue engineering: in vitro and in vivo assessment of biological performance. Acta Biomater 2015;12:227–41.

[22] McMahon LA, O'Brien FJ, Prendergast PJ. Biomechanics and mechanobiology in osteochondral tissues. Regen Med 2008; 3(5):743–59.

[23] Liebschner MAK. Biomechanical considerations of animal models used in tissue engineering of bone. Biomaterials 2004; 25(9):1697–714.

[24] Pan Z, Duan PG, Liu XN, Wang HR, Cao L, He Y, et al. Effect of porosities of bilayered porous scaffolds on spontaneous osteochondral repair in cartilage tissue engineering. Regen Biomater 2015;2(1):9–19.

[25] Jing DY, Wu LB, Ding JD. Solvent-assisted room-temperature compression molding approach to fabricate porous scaffolds for tissue engineering. Macromol Biosci 2006;6(9):747–57.

[26] Zhang JC, Wu LB, Jing DY, Ding JD. A comparative study of porous scaffolds with cubic and spherical macropores. Polymer 2005;46(13):4979–85.

[27] Zhou J, Lin H, Fang TL, Li XL, Dai WD, Uemura T, et al. The repair of large segmental bone defects in the rabbit with vascularized tissue engineered bone. Biomaterials 2010;31(6): 1171–9.

[28] Wakitani S, Goto T, Pineda SJ, Young RG, Mansour JM, Caplan AI, et al. Mesenchymal cell-based repair of large, full-thickness defects of articular-cartilage. J Bone Joint Surg Am Vol 1994;76a(4):579–92.

[29] Chen JW, Wang CY, Lu SH, Wu JZ, Guo XM, Duan CM, et al. In vivo chondrogenesis of adult bone-marrow-derived autologous mesenchymal stem cells. Cell Tissue Res 2005;319(3): 429–38.

[30] Wu LB, Ding JD. Effects of porosity and pore size on in vitro degradation of three-dimensional porous poly(D,L-lactide-co-glycolide) scaffolds for tissue engineering. J Biomed Mater Res A 2005;75(4):767–77.

[31] Huang X, Yang D, Yan WQ, Shi ZL, Feng J, Gao YB, et al. Osteochondral repair using the combination of fibroblast growth factor and amorphous calcium phosphate/poly(L-lactic acid) hybrid materials. Biomaterials 2007;28(20): 3091–100.

[32] Chen JN, Chen H, Li P, Diao HJ, Zhu SY, Dong L, et al. Simultaneous regeneration of articular cartilage and subchondral bone in vivo using MSCs induced by a spatially controlled gene delivery system in bilayered integrated scaffolds. Biomaterials 2011;32(21):4793–805.

[33] Mok SW, Nizak R, Fu SC, Ho KK, Qin L, Saris DBF, et al. From the printer: potential of three-dimensional printing for orthopaedic applications. J Orthop Translat 2016;6:42–9.

[34] Zhu M, Feng Q, Sun Y, Li G, Bian L. Effect of cartilaginous matrix components on the chondrogenesis and hypertrophy of mesenchymal stem cells in hyaluronic acid hydrogels. J Biomed Mater Res B Appl Biomater 2017;105(8):2292–300.

[35] Feng Q, Lin S, Zhang K, Dong C, Wu T, Huang H, et al. Sulfated hyaluronic acid hydrogels with retarded degradation and enhanced growth factor retention promote hMSC chondrogenesis and articular cartilage integrity with reduced hypertrophy. Acta Biomater 2017;53:329–42.

[36] Li R, Xu J, Wong DSH, Li J, Zhao P, Bian L. Self-assembled N-cadherin mimetic peptide hydrogels promote the chondrogenesis of mesenchymal stem cells through inhibition of canonical Wnt/beta-catenin signaling. Biomaterials 2017;145: 33–43.

[37] Zhu Y, Liu D, Wang X, He Y, Luan W, Qi F, et al. Polydopamine-mediated covalent functionalization of collagen on a titanium alloy to promote biocompatibility with soft tissues. J Mater Chem B 2019;7(12):2019–31.

[38] Lee WY, Wang B. Cartilage repair by mesenchymal stem cells: clinical trial update and perspectives. J Orthop Translat 2017; 9:76–88.

[39] Peng YM, Liu QJ, He TL, Ye K, Yao X, Ding JD. Degradation rate affords a dynamic cue to regulate stem cells beyond varied matrix stiffness. Biomaterials 2018;178:467–80.

[40] Zhen GH, Wen CY, Jia XF, Li Y, Crane JL, Mears SC, et al. Inhibition of TGF-beta signaling in mesenchymal stem cells of subchondral bone attenuates osteoarthritis. Nat Med 2013; 19(6):704–12.

[41] Zhen GH, Cao X. Targeting TGFbeta signaling in subchondral bone and articular cartilage homeostasis. Trends Pharmacol Sci 2014;35(5):227—36.

[42] O'Reilly A, Kelly DJ. A computational model of osteochondral defect repair following implantation of stem cell-laden multiphase scaffolds. Tissue Eng 2017;23(1—2):30—42.

[43] Shao XX, Goh JCH, Hutmacher DW, Lee EH, Ge ZG. Repair of large articular osteochondral defects using hybrid scaffolds and bone marrow-derived mesenchymal stem cells in a rabbit model. Tissue Eng 2006;12(6):1539—51.

[44] Jiang CC, Chiang H, Liao CJ, Lin YJ, Kuo TF, Shieh CS, et al. Repair of porcine articular cartilage defect with a biphasic osteochondral composite. J Orthop Res 2007;25(10):1277—90.

[45] Vindas Bolanos RA, Cokelaere SM, Estrada McDermott JM, Benders KE, Gbureck U, Plomp SG, et al. The use of a cartilage decellularized matrix scaffold for the repair of osteochondral defects: the importance of long-term studies in a large animal model. Osteoarthritis Cartilage 2017;25(3):413—20.